Macromolecules

ARTICLE

pubs.acs.org/Macromolecules

Synthesis of Linear and Star-Shaped Poly[4-(diphenylamino)benzyl methacrylate]s by Group Transfer Polymerization and Their Electrical Memory Device Applications

Jung-Ching Hsu,[†,∥] Yougen Chen,[‡,∥] Toyoji Kakuchi,[*,‡] and Wen-Chang Chen[*,†,§]

[†]Department of Chemical Engineering, National Taiwan University, Taipei 10617, Taiwan

[‡]Graduate School of Chemical Sciences and Engineering, Faculty of Engineering, Hokkaido University, Sapporo 060-8628, Japan

[§]Institute of Polymer Science and Engineering, National Taiwan University, Taipei 10617, Taiwan

Supporting Information

ABSTRACT: Hole-transporting triphenylamine (TPA)-based polymers, the linear poly[4-(diphenylamino)benzyl methacrylate] (PTPMA) and the three-armed star-shaped poly[4-(diphenylamino)benzyl methacrylate] ($N(PTPMA)_3$), have been synthesized by group transfer polymerization (GTP). For the synthesis of $N(PTPMA)_3$, the core-first approach coupled with the GTP was adopted using a newly designed silyl ketene acetal initiator with three initiating points. The polymerization results showed that the polymer molecular weights were precisely controlled by the monomer/initiator ratio. The new hole-transporting TPA-based polymers could be blended with electron-accepting [6,6]-phenyl-C_{61}-butyric acid methyl ester (PCBM) for electrical memory device applications. The experimental results showed that pristine PTPMA and $N(PTPMA)_3$ exhibited dynamic-random-access-memory (DRAM) volatile electrical behavior, but their PCBM composite-based devices changed to the write-once-read-many times (WORM) nonvolatile memory characteristic or conductor behavior. The ON or OFF state for the WORM memory devices could remain over 10^4 s without any degradation. The optical absorption and photoluminescence results indicated that the charge transfer complexation between the TPA and PCBM led to the varied PCBM aggregated size and memory characteristics. The trapping-detraping and field-induced charge transfer effects were used to explain the different memory characteristics. The steric hindrance of the star-shaped $N(PTPMA)_3$ compared to PTPMA probably reduced the electron transport efficiency from Al to the LUMO of PCBM in the polymer/PCBM composite-based devices, such as turn-on voltage and conduction mechanism. The present study reveals the importance of polymer architecture or donor/acceptor composition on tuning memory device characteristics.

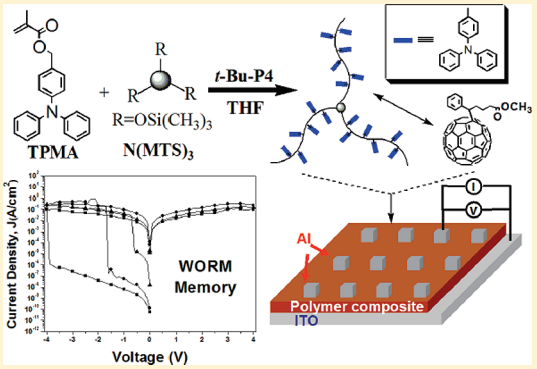

INTRODUCTION

Polymer nanocomposites derived from nanomaterials significantly affected the charge transport processes between the electrodes for electrical memory device applications, such as carbon nanotube,[1,2] fullerene,[3−6] metal nanoparticle,[7−9] and graphene oxide.[10] The switching mechanisms of the polymer composites were explained by charge transfer, charge trapping, and filament conduction summarized by Kang and co-workers.[11,12] Functional block copolymer composites were used to control fullerene domain size through specified physical interaction.[5] For example, we prepared supramolecular composite thin films of poly[4-(9,9-dihexylfloren-2-yl)styrene]-*block*-poly(2-vinylpyridine) (P(St-Fl)-*b*-P2VP):[6,6]-phenyl-C_{61}-butyric acid methyl ester (PCBM) for write-once-read-many times (WORM) nonvolatile memory devices.[5] Thus, design and synthesize functional polymers could be very important in controlling the composite morphology for electrical memory device applications.

Polymers with pendent π-conjugated moieties have been extensively studied due to the precisely conjugation length and optoelectronic properties, structural flexibility, and processability.[13−19] For instance, polymers with pendent triphenylamine (TPA) moiety are known as attractive hole-transport materials for electrical memory device.[20−24] The electrical memory behaviors of the TPA-acceptor polyimides (PIs) could be tuned by different electron-withdrawing moieties, including dynamic random access memory (DRAM), static random access memory (SRAM), and write-once-read-many times (WORM).[25−29] Thus, well-defined polymers with pendent TPA moiety were synthesized using various living polymerization methods, such as anionic[30−33] and radical polymerization.[22,34,35] However, the synthesis of star-branched polymers with the TPA moiety is rarely explored. Recently, we

Received: March 20, 2011
Revised: May 27, 2011
Published: June 07, 2011

Scheme 1. Synthetic Route for Linear PTPMA and Three-Armed Star-Shaped N(PTPMA)$_3$

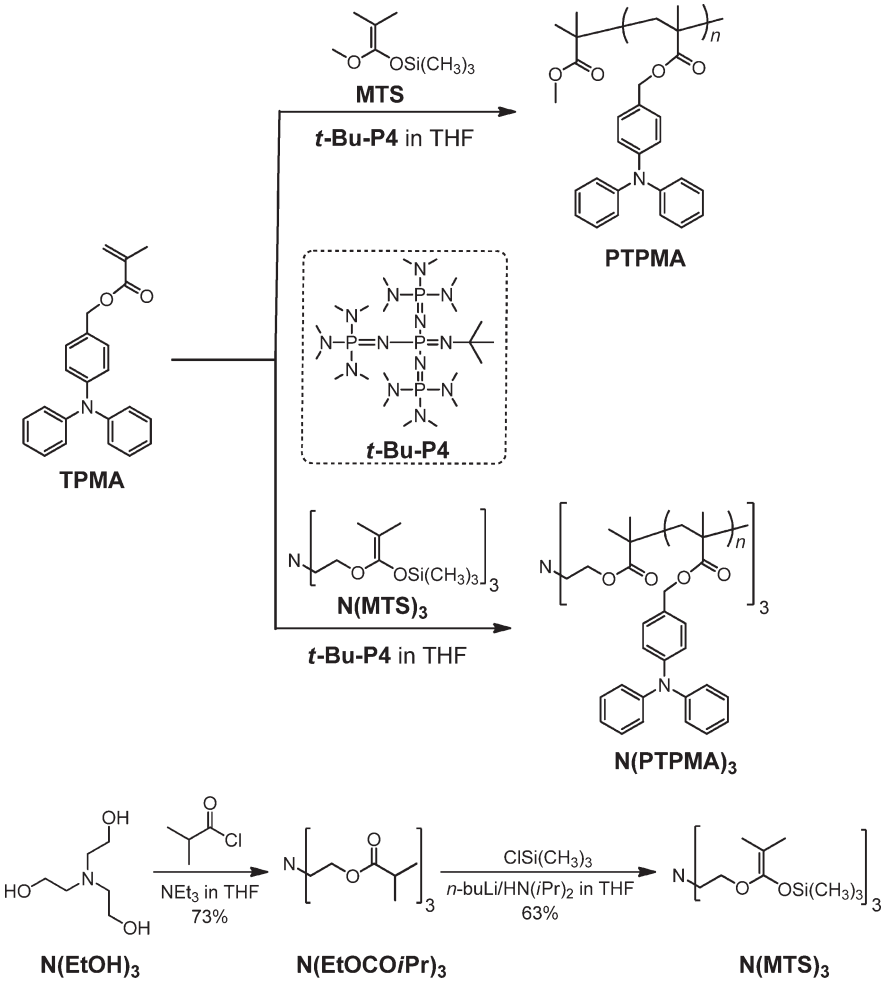

reported that the group transfer polymerization (GTP) of methacrylate and acrylamide derivatives using a silyl ketene acetal as an initiator, which allowed for excellent molecular weight control, narrow molecular weight distribution, and specialized polymer chain architecture.[36−40] Thus, it would be of significant interest to design and precisely synthesize well-defined macromolecular architectures containing the TPA moiety by the GTP of methacrylate derivatives.

In this study, we report the synthesis of linear and star-shaped PTPMAs by the GTP method (Scheme 1). For the synthesis of the three-armed star-shaped N(PTPMA)$_3$, we prepared through the core-first approach with a newly designed silyl ketene acetal possessing three initiating points as the initiator and phosphazene base, *t*-Bu-P4, as the catalyst. The memory device characteristics with a device configuration of ITO/composite/Al based on PTPMA or N(PTPMA)$_3$ and their PCBM composite films were explored. The interaction between the studying polymers and PCBM was investigated by optical absorption and photoluminescence (PL) spectra. The morphology of the prepared composites was characterized by transmission electron microscopy (TEM) and atom force microscopy (AFM). The appropriate conduction model was used to analyze the obtained current density−voltage ($J-V$) curves. The experimental results suggested that the significance of polymer architecture or donor/acceptor composite ratios on the memory characteristics.

EXPERIMENTAL SECTION

Materials. 4-(*N*,*N*-Diphenylamino)benzaldehyde (>98%) was purchased from Tokyo Kasei Kogyo Co., Ltd., Japan (TCI). Sodium borohydryde was provided by Kanto Chemical Co., Inc., and used as received. Methacryloyl chloride (>80%) was available from TCI and distilled under reduced pressure prior to use. Triethanolamine (>99%, Sigma-Aldrich) and isobutyryl chloride (>98%, TCI) were distilled under reduced pressure prior to use. The 1-methoxy-1-trimethylsilyloxy-2-methylpropene (MTS) was purchased from TCI and used after distillation under reduced pressure without drying agent. *t*-Bu-P4 base (1.0 mol L^{-1} in hexane) was purchased from Sigma-Aldrich Chemicals Co., Inc., and used as received. Dimethylaminopyridine (DMAP, >99%) was purchased from Wako Pure Chemical Industrial. Ltd. Triethylamine (>99%) was available from Kanto Chemical Co., Inc., and distilled before use. Tetrahydrofuran (THF, >99.5%, dehydrated stabilizer free) was provided by Kanto Chemical Co., Inc., and distilled over Na/benzophenone under an argon atmosphere for polymerization usage. [6,6]-Phenyl-C_{61}-butyric acid methyl ester (PCBM) was obtained from Nano-C Inc. All other reagents are used as received unless further instruction.

Characterization. The ^{1}H and ^{13}C NMR spectra were recorded on JEOL JNM-A400II and JEOL-ECP-400 instruments. Polymerization was carried out in an MBRAUN stainless steel glovebox equipped with a gas purification system (molecular sieves and copper catalyst) in a dry argon atmosphere (H_2O, O_2 <1 ppm). The moisture and oxygen

contents in the glovebox were monitored by an MB-MO-SE 1 and an MB-OX-SE 1, respectively. The size exclusion chromatography (SEC) was performed at 40 °C in THF (1.0 mL min^{-1}) using a Jasco GPC-900 system equipped with set of Waters Ultrastyragel 7 mm columns (linear, 7.8 mm × 300 mm) and two Shodex KF-804 L columns (linear, 8 mm × 300 mm). The number-average molecular weight (M_n) and polydispersity index (M_w/M_n) of the polymers were calculated on the basis of polystyrene standards. UV−vis optical absorption and photoluminescence (PL) spectra were obtained using a Hitachi U-4100 spectrometer and Fluorolog-3 spectrofluorometer (Jobin Yvon), respectively. Electrochemical analysis was performed with a CHI 611B electrochemical analyzer using an ITO plate as working electrode, platinum wire as counter electrode, and Ag/AgCl as reference electrode at a sweep rate 0.1 V s^{-1}. A 0.1 M solution of tetrabutylammonium perchlorate (TBAP) in anhydrous acetonitrile was employed as the supporting electrolyte. The thickness of polymer film was measured with a Microfigure Measuring Instrument (Surfcorder ET3000, Kosaka Laboratory Ltd.). The morphologies of polymer film surface was obtained with a Nanoscope 3D Controller atomic force micrographs (AFM, Digital Instruments) operated in the tapping mode at room temperature. The electrical characterization of the memory device was performed by a Keithley 4200-SCS semiconductor parameter analyzer in a glovebox (O_2 <1 ppm, H_2O <1 ppm). ITO was used as the cathode (maintained as common), and Al was set as the anode during the voltage sweep. The probe tip used 10 μm diameter tungsten wire attached to a tinned copper shaft with a point radius <0.1 μm (GGB Industries, Inc.).

Synthesis of 4-(Diphenylamino)benzyl Methacrylate (TPMA). To a mixture of 4-(diphenylamino)benzyl alcohol (8.00 g, 29.10 mmol), DMAP (0.18 g, 1.46 mmol), and triethylamine (6.10 mL, 43.65 mmol) in THF, methacryloyl chloride (3.70 mL, 34.92 mmol) was slowly added at 0 °C under an argon atmosphere. The reaction was stirred for 72 h at room temperature. Then, the mixture was filtered to remove an insoluble salt, and residual filtrate was evaporated. After being dissolved in CH_2Cl_2, the residue was washed with saturated $NaHCO_3$ and aqueous NaCl solution. The organic layer was evaporated to remove solvent, followed by drying over anhydrous Na_2SO_4. The resultant oily liquid was purified by column chromatography (silica gel, toluene). Toluene was evaporated under reduced pressure, and the product was vacuumed overnight to give a colorless oily liquid. Yield = 8.45 g (85%). ^{1}H NMR (400 MHz, $CDCl_3$, δ): 1.98 (s, 3H, $-CH_3$), 5.13 (s, 2H, $-CH_2$), 5.58 (d, 1H, $=CH$), 6.18 (s, 1H, $=CH$), 6.98−7.36 (m, 14H, aromatic H). ^{13}C NMR (100 MHz, $CDCl_3$, δ): 166.9 (1C, C=O), 147.3 (aromatic C), 135.9 (1C, CH_2=C), 129.8 (aromatic C), 129.0 (aromatic C), 125.3 (aromatic C), 124.5 (aromatic C), 122.5 (1C, CH_2=C), 122.3 (aromatic C), 65.7 (1C, $-CH_2-$), 17.9 (1C, $-CH_3$). Anal. Calcd for $C_{23}H_{21}NO_2$ (343.18): C, 80.44; H, 6.16; N, 4.08. Found: C, 80.66; H, 6.16; N, 4.09.

Synthesis of 2,2′,2″-Nitrilotris(ethane-2,1-diyl)tris(2-methylpropanoate) (N(EtOCO*i*Pr)$_3$). To the mixture of triethanolamine ($N(EtOH)_3$) (7.46 g, 50.00 mmol) and triethylamine (31.20 mL, 225.00 mmol) in dry THF (120 mL), isobutyryl chloride (19.20 mL, 180.00 mmol) was slowly dropwised at 0 °C under an nitrogen atmosphere. After the reaction was stirred at room temperature overnight, the mixture was dissolved in ethyl acetate and washed with saturated aqueous $NaHCO_3$, aqueous NaCl, and water. The organic layer was dried over anhydrous Na_2SO_4 and then evaporated to remove the solvent. The residue was distilled (124 °C, 16 Pa) and then purified by column chromatography (silica gel, dichloromethane → ethyl acetate) to give $N(EtOCOiPr)_3$ as a lightly yellow liquid. Yield = 13.16 g (73%). ^{1}H NMR (400 MHz, $CDCl_3$, δ): 4.07 (t, 6H, $-CH_2-O-$), 2.81 (t, 6H, $-O-CH_2-CH_2-$), 2.55 (m, 3H, $-CH_3-CH-$), 1.18 (d, 18H, CH_3-CH-).

Synthesis of Tris(2-(2-methyl-1-(trimethylsilyloxy)prop-1-enyloxy)ethyl)amine (N(MTS)$_3$). Anhydrous THF (25 mL) and degassed diisopropylamine (3.00 mL, 21.40 mmol) were added to a 100 mL cock-attached flask under an argon atmosphere. The obtained solution was cooled to 0 °C and *n*-butyllithium (8.6 mL, 21.4 mmol; 2.5 M in hexane) was added dropwise. After stirring for 1 h, $N(EtOCOiPr)_3$ (2.40 g, 21.4 mmol) was slowly added, and the temperature was cooled to −78 °C. The reaction mixture was stirred for 1 h, and then trimethylsilyl chloride (6.5 mL, 51.2 mmol) was added dropwise. The mixture was warmed to room temperature and stirred overnight. The solvent was removed under reduced pressure, and the residue was distilled (140 °C, 48 pa) to give $N(MTS)_3$ as a colorless liquid. Yield = 2.44 g (63%). ^{1}H NMR (400 MHz, $CDC1_3$): 3.78 (t, 6H, $-CH_2-O-$), 2.80 (t, 6H, $-O-CH_2-CH_2-$), 1.58 (d, 18 H, $C-CH_3$), 0.50 (s, 27 H, $Si-CH_3$).

Synthesis of Linear PTPMA. TPMA was diluted to be a solution (0.40 mol L^{-1}). Before polymerization, the obtained solution was stirred over CaH_2 (without stabilizer) overnight and then filtered through a 0.45 μm PTFE syringe filter. Here, the feed ratio of $[TPMA]_0/[MTS]_0/[t\text{-Bu-P4}]_0$ = 40/1/0.03 was typically taken as an example. The polymerization was carried out as follows: in glovebox, after MTS solution (25 μL, 5 μmol; 0.20 mol L^{-1}) and *t*-Bu-P4 solution (75 μL, 0.15 μmol; 0.0020 mol L^{-1}) were sequentially added to a test tube. The mixture was stirred for a few minutes. Then, a TPMA solution (0.50 mL, 200 μmol; 0.40 mol L^{-1}) was added dropwise to start the polymerization. After 30 min, an excessive benzoic acid was added to quench the polymerization. The reaction mixture was poured into a large amount of methanol, followed by drying in vacuo to give a white solid. Yield = 121 mg (88%). Conversion >99%, $M_{n,SEC}$ = 9900, M_w/M_n = 1.13; $M_{n,NMR}$ = 13 700. ^{1}H NMR (400 MHz, $CDC1_3$, δ): 6.80−7.24 (broad, aromatic H), 4.65−5.00 (broad, TPA−CH_2OOC−), 3.56 (broad, CH_3OOC−), 1.20−2.20 (broad, $-CCH_3-CH_2-$) 0.60−1.20 (broad, $-CCH_3-CH_2-$).

Synthesis of Three-Armed N(PTPMA)$_3$. A typical polymerization is as follows: in glovebox, an $N(MTS)_3$ solution (100 μL, 20 μmol; 0.20 mol L^{-1} in THF) and a *t*-Bu-P4 solution (0.30 mL, 0.60 μmol; 0.0020 mol L^{-1} in THF) were sequentially added to a test tube, and the mixture was stirred for a few minutes. Then, a TPMA solution (1.50 mL, 0.60 mmol; 0.40 mol L^{-1} in THF) was added dropwise to start the polymerization. After 30 min, an excessive benzoic acid was added to quench the polymerization. The reaction mixture was poured into a large amount of methanol, followed by drying in vacuum to give a white solid. Yield = 159.3 mg (77%). Conversion >99.9%, $M_{n,SEC}$ = 6200, M_w/M_n = 1.10; $M_{n,NMR}$ = 11 100. ^{1}H NMR (400 MHz, $CDC1_3$, δ): 6.80−7.24 (broad, aromatic H), 4.65−5.00 (broad, TPA−CH_2OOC−), 3.98 (broad, $-NCH_2CH_2OOC-$), 2.76 (broad, $-NCH_2CH_2OOC-$), 1.20−2.20 (broad, $-CCH_3-CH_2-$) 0.60−1.20 (broad, $-CCH_3-CH_2-$).

Fabrication of Polymer Memory Devices. The electrical properties of memory devices were fabricated with the configuration of ITO/polymer/Al, which is similar to our previous study.[28,33] The PCBM was dissolved in chloroform solution at a concentration of 1 mg mL^{-1}. A chloroform solution of polymer (5 mg mL^{-1}), containing a calculated amount of PCBM, was stirred overnight to form homogeneous solutions. Thereafter, the solution was filtered through 0.22 μm pore size of PTFE membrane syringe filter. The filtered solutions were spin-coated at 500 rpm for 30 s onto the ITO substrate. The polymer thin films were dried under vacuum (10^{-6} Torr) for 2 h to remove all of the solvents used. The thickness of the prepared thin film was estimated to be around 50 nm. Finally, the 200 nm thick Al top electrode was thermally evaporated through the shadow mask at a pressure of 10^{-6} Torr with a slow deposition rate (1.2−1.3 Å/s^{-1}) to avoid the penetration of Al into the polymer layer. The active device area was recorded about 0.5 × 0.5 mm^2 in size.

RESULTS AND DISCUSSION

Synthesis of Linear PTPMA. The molecular weight was controlled by varying the $[TPMA]_0/[MTS]_0$ ratios, as listed in

Table 1. Synthesis of Linear PTPMA by *t*-Bu-P4-Catalyzed GTP of TMPA Using MTS[a]

run	$[TPMA]/[MTS]_0$	conv[b] (%)	$M_{n,theo}$[c]	$M_{n,NMR}$[d]	DP[d]	$M_{n,SEC}$ (M_w/M_n)[e]
1	20	>99	6900	6200	18	5000 (1.26)
2	30	>99	10300	10300	30	7500 (1.13)
3	40	>99	13700	13700	40	9900 (1.13)
4	50	>99	17200	17200	50	11000 (1.09)
5	100	>99	34300	34000	99	20000 (1.06)

[a] Ar atmosphere; solvent, THF; temperature, room temperature; $[TPMA]_0 = 0.40$ mol L^{-1}; $[t\text{-Bu-P4}]_0/[MTS]_0 = 0.03$; time, 0.5 h. [b] Determined by ^1H NMR in $CDCl_3$. [c] $M_{n,theo} = [TPMA]_0/[MTS]_0 \times$ (MW of TPMA) + (MW of $MTS_{residual}$). [d] Determined by ^1H NMR in $CDCl_3$, $M_{n,NMR} = DP \times$ (MW of TPMA) + (MW of $MTS_{residual}$). [e] Determined by SEC using PSt standards in THF.

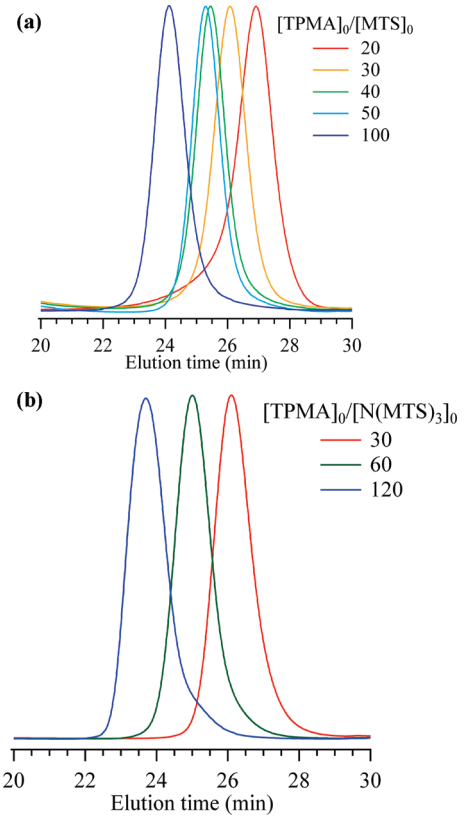

Figure 1. SEC traces of $N(PTPMA)_3$s with various (a) $[TPMA]_0/[MTS]_0$ ratios and (b) $[TPMA]_0/[N(MTS)_3]_0$ ratios determined in THF using polystyrene standards.

Table 1. The $[TPMA]_0/[MTS]_0$ ratios were fixed in the range from 20 to 100, and all other conditions were set to be the same. The polymerization proceeded so fast that conversions of all polymerizations reached ca. 100% within 30 min. With the increase of $[TPMA]_0/[MTS]_0$, the number-average molecular weights estimated from SEC ($M_{n,SEC}$) increased and were estimated in the range of 5000−20 000, with the estimated M_w/M_n of 1.06−1.26, as shown in Figure 1a. All the SEC traces exhibited a unimodal shape and narrow distribution. Moreover, the SEC trace displayed an obvious shift to a higher molecular weight region corresponding to the increase of $[TPMA]_0/[MTS]_0$ value. The DPs calculated from ^1H NMR spectrum ranged from 18 to 99, which were in good accordance with $[TPMA]_0/[MTS]_0$ ratios in feed. Meanwhile, the molecular weights estimated from ^1H NMR spectrum ($M_{n,NMR}$) were between 6200 and 34 000, which fairly agreed with the theoretical molecular weights ($M_{n,th}$s). Figure S1(a) of the Supporting Information shows the ^1H NMR spectrum of the obtained polymer (run 2). The signal due to the methoxy protons as the end functional group derived from MTS is clearly observed at 3.56 ppm, and the signals due to the methylene proton from the main chain and the methyl group in the side group are observed between the ranges of 1.20−2.20 ppm (peak b) and 0.60−1.20 ppm (peak a), respectively. The signals at 4.65−5.00 ppm (peak c) and 6.80−7.24 ppm (peak d) are attributed to the methylene and aromatic protons from the side group.

Synthesis of Star-Shaped $N(PTPMA)_3$. In order to synthesize the three-armed star-shaped polymers by GTP, a newly designed $N(MTS)_3$ was prepared as the core-first initiator. Similar to the synthesis of linear PTPMA, the $[TPMA]_0/[N(MTS)_3]_0$ ratios were fixed from 30 to 120. The polymerization results are summarized in Table 2. The monomers quantitatively consumed within 30 min for all polymerization systems. The $M_{n,SEC}$ values were ranged from 6200 to 18 000, corresponding to the $[TPMA]_0/[N(MTS)_3]_0$ ratios in feed. The M_w/M_ns calculated by SEC measurements were in the range of 1.09−1.10. All of the SEC traces shown in Figure 1b exhibited a unimodal shape. Moreover, the SEC trace displayed an obvious shift to a higher molecular weight region corresponding to the increase of $[TPMA]_0/[N(MTS)_3]_0$ value. The DPs calculated from the ^1H NMR spectrum ranged from 31 to 120, which were in good accordance with $[TPMA]_0/[N(MTS)_3]_0$ ratios in feed. Meanwhile, the molecular weights estimated from ^1H NMR spectrum ($M_{n,NMR}$) were between 11 100 and 41 600, which fairly agreed with the $M_{n,th}$s. For the ^1H NMR spectrum of $N(PTPMA)_3$ (run 6), the proton signal derived from the $N(MTS)_3$ residue was clearly observed at 2.76 and 3.98 ppm in Figure S1(b) of the Supporting Information, and the proton signals due to the monomer unit were also clearly observed as well as the linear PTPMA.

Characterization of Linear PTPMA and Star-Shaped $N(PTPMA)_3$. The linear PTPMA with $M_{n,SEC} = 7500$ g/mol, $M_w/M_n = 1.13$ (run 2) and three-armed star-shaped $N(PTPMA)_3$ with $M_{n,SEC} = 6200$ g/mol, $M_w/M_n = 1.10$ (run 6) were used for memory device fabrication. In the absorption spectra for thin films of PTPMA and $N(PTPMA)_3$ (Figure 2a), the absorption maximum for both thin films exhibits a similar value around 305 nm, attributed to the $\pi-\pi^*$ transition of the triphenylamine moiety in the polymer chain.[41] The optical band gap (E_g^{opt}) determined by the onset absorption edge (observed at 345 nm) is around 3.60 eV. The onset oxidation potentials (E_{onset}^{ox}) estimated from the cyclic voltammetry (CV) curve for the thin films of the PTPMA and $N(PTPMA)_3$ are 0.98 and 1.02 eV, respectively, as shown in Figure 2b. The HOMO energy level was determined from E_{onset}^{ox} and estimated on the basis of the reference energy level of ferrocence (4.8 eV) below the vacuum level. The relationship is shown by the following equations:

dx.doi.org/10.1021/ma2006377 |*Macromolecules* 2011, 44, 5168–5177

Table 2. Synthesis of N(PTPMA)$_3$s by *t*-Bu-P4-Catalyzed GTP of TPMA Using N(MTS)$_3$[a]

run	$[TPMA]_0/[N(MTS)_3]_0$	conv[b] (%)	$M_{n,theo}$[c]	$M_{n,NMR}$[d]	DP[d]	$M_{n,SEC}$ (M_w/M_n)[e]
6	30	>99	10700	11100	31	6200 (1.10)
7	60	>99	21000	21300	61	9700 (1.09)
8	120	>99	41600	41600	120	18000 (1.10)

[a] Ar atmosphere; solvent, THF; temperature, room temperature; $[TPMA]_0$ = 0.40 mol L^{-1}; $[N(MTS)_3]_0/[t\text{-Bu-P4}]_0$ = 1/0.03; time, 0.5 h. [b] Determined by ^1H NMR in $CDCl_3$. [c] $M_{n,theo} = [TPMA]_0/[N(MTS)_3]_0 \times$ (MW of TPMA) + (MW of $N(MTS)_{3,residual}$). [d] Determined by ^1H NMR in $CDCl_3$, $M_{n,NMR}$ = DP × (MW of TPMA) + (MW of $N(MTS)_{3,residual}$). [e] Determined by SEC using PSt standards in THF.

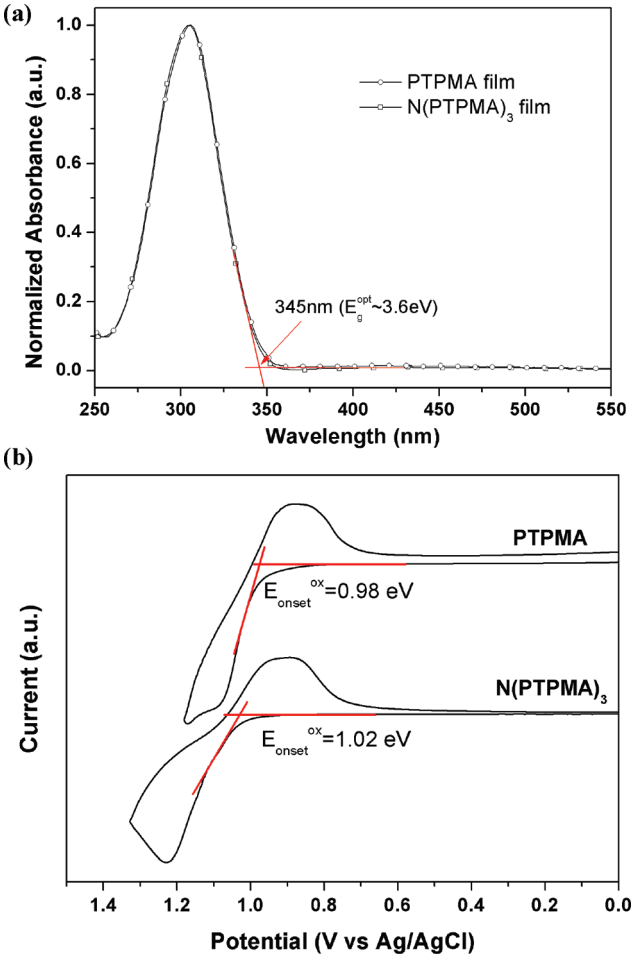

Figure 2. (a) Optical absorption spectra of the PTPMA and N(PTPMA)$_3$ thin films. (b) Cyclic voltammograms of PTPMA and N(PTPMA)$_3$ in 0.1 M TBAP/acetonitrile solution.

HOMO (eV) = $-e(E_{ox}^{onset} - E_{1/2,ferrocene} + 4.8$ eV). Besides, the LUMO energy level was determined by the difference between HOMO level and E_g^{opt} based on the following equation: LUMO (eV) = HOMO + E_g^{opt}.[29] Therefore, the HOMO and LUMO energy levels of PTPMA (run 2) and N(PTPMA)$_3$ (run 6) were estimated to be (−5.30, −1.70) eV and (−5.34, −1.74) eV, which showed an insignificant variation with the polymer architecture.

Characterization of PCBM:Polymer Composites. The interaction between PCBM and polymers, PTPMA and N(PTPMA)$_3$, was probed by absorption and photoluminescence spectra, as shown in Figure 3. The absorption spectra of the PCBM:N(PTPMA)$_3$ thin films are shown in Figure 3a. The absorption edge extended into the long-wavelength range with the enhanced

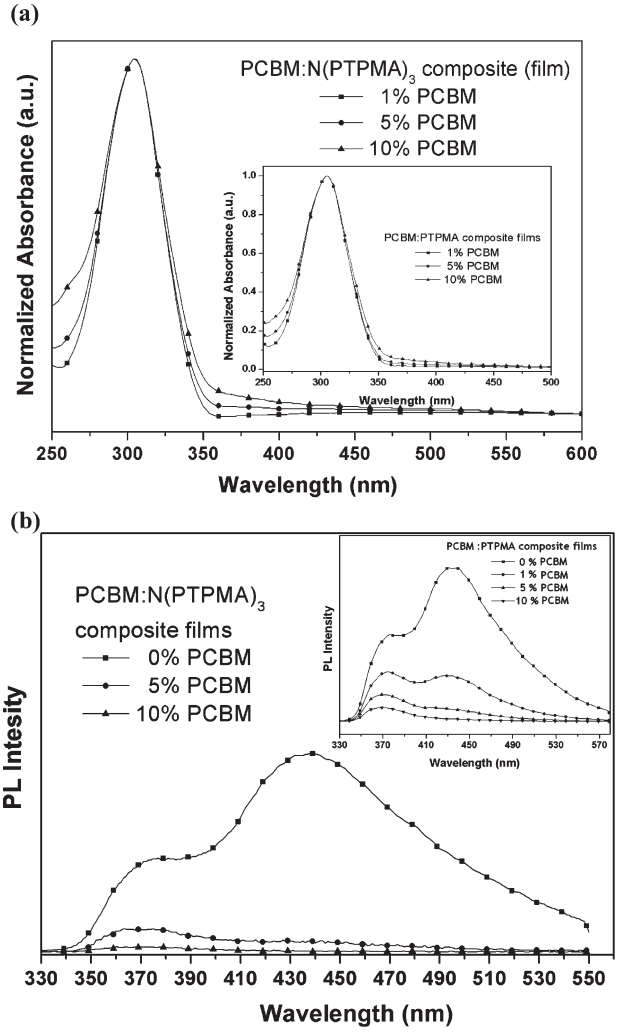

Figure 3. (a) Optical absorption spectra of the PCBM:N(PTPMA)$_3$ composite thin films. (b) Photoluminescence spectra of PCBM:N(PTPMA)$_3$ thin films.

PCBM composition from 1 to 10 wt %, implying that the PCBM and N(PTPMA)$_3$ forms charge transfer complex in the solid state and extended the delocalization of the triphenylamine moieties.[9] The interaction between N(PTPMA)$_3$ and PCBM was further characterized by photoluminescence (PL) spectra of the composite films, as exhibited in Figure 3b. The PL spectra of pristine N(PTPMA)$_3$ thin film exhibit a strong emission peak located at (377, 438) nm. The peak at 438 nm is due to the excimer formation between the triphenylamine moieties.[42−44] The emission intensity of the PL spectra is almost quenched by adding 10% PCBM, which is also an evidence for charge transfer formation.

dx.doi.org/10.1021/ma2006377 |*Macromolecules* 2011, 44, 5168–5177

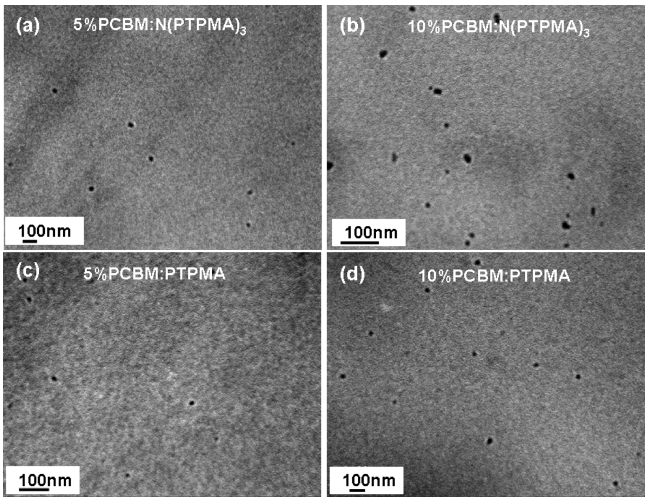

Figure 4. TEM images of (a) 5% PCBM:N(PTPMA)$_3$, (b) 10% PCBM:N(PTPMA)$_3$, (c) 5% PCBM:PTPMA, and (d) 10% PCBM:PTPMA composite thin films.

Besides, similar results on the results of the absorption edge and PL quenched are also observed in PCBM:PTPMA composite films, as shown in the inset of Figure 3.

The TEM images of the PCBM:N(PTPMA)$_3$ and PCBM:PTPMA composite films are shown in Figure 4. The domain size of PCBM clusters was estimated by averaging the dark domains, which most likely correspond to PCBM clusters in the PCBM:polymer composite films.[45] The sizes of PCBM clusters are around 12 and 15 nm for 5% and 10% PCBM:N(PTPMA)$_3$, respectively, while 13 and 35 nm are observed for 5% and 10% PCBM:PTPMA. The interaction between the electron-accepting PCBM and electron-donating TPA moieties plays a key role in controlling the PCBM domain size in the polymer matrix.[46] Such difference on the PCBM aggregation size affects the switching characteristic significantly. The AFM height images of the PCBM:N(PTPMA)$_3$ and PCBM:PTPMA composite films on ITO surface are shown in Figure S2 of the Supporting Information. The composite films through conventional solution spin-coating processes exhibit smooth surface with small root-mean-square values around 0.7−1.1 nm.

Memory Performance Based on PCBM:Polymer Composite Devices. The current density−voltage (J−V) curves of the memory devices, ITO/N(PTPMA)$_3$/Al, are shown in Figure 5a, where the polymer film thickness is around 50 nm. The electrical properties of pristine N(PTPMA)$_3$ is initially in the low conductivity state with a current density in the range of 10^{-10}−10^{-11} (A cm^{-2}) during the voltage swept from 0 to −3.0 V. The current density increases abruptly at a threshold voltage −3.1 V and changes from the OFF state to ON state as the "writing" process (first sweep). Besides, the ON state remains during the repeated voltage sweep from 0 to −4 V and the ON/OFF current ratio at −1 V is as high as 10^8 (second sweep). The memory device returns to the OFF state for a period of 1 min after turning off the power and could be reprogrammed from the OFF state to the ON state again with a threshold voltage of −2.8 V and kept in the ON state (the third and fourth sweeps), indicating that the device is rewritable. The J−V curves exhibiting the volatile property can be measured in at least 10 devices with reproduced data. This unstable ON state can be maintained by a refreshing voltage pulse of −1 V of 1 ms duration every 5 s (named the rf

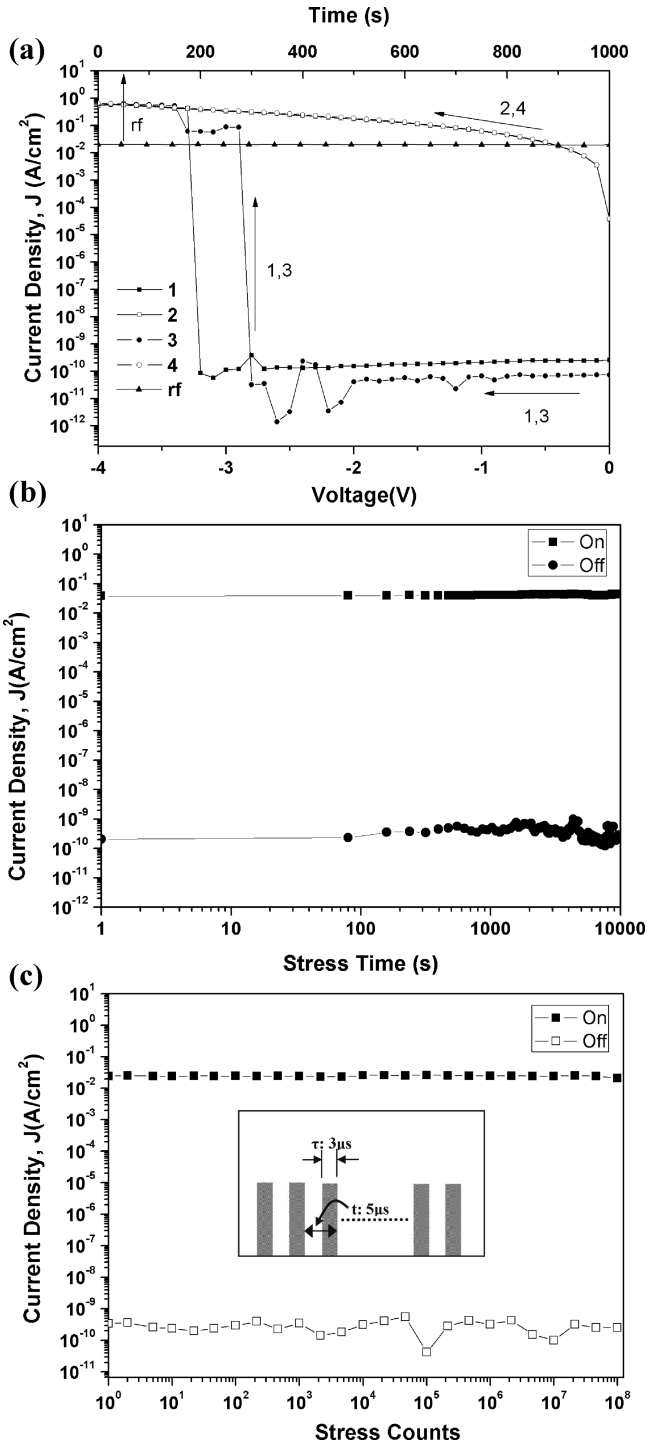

Figure 5. (a) Current density−voltage curves for ITO/N(PTPMA)$_3$/Al devices. (b) Retention times of the ITO/N(PTPMA)$_3$/Al device. (c) Stimulus effect of read pulses on the ON and OFF states of the ITO/N(PTPMA)$_3$/Al device.

trace). For the retention times and stress tests of both the ON and OFF states of N(PTPMA)$_3$, the device initially starts to turn ON or OFF to a high or low conductivity state. Under a constant stress of −1 V, no obvious degradation in current is observed for both ON and OFF states for at least 10^4 s during the readout test as shown in Figure 5b. The stimulus effect of read pulses on the ON and OFF state was also investigated for the long time test.

dx.doi.org/10.1021/ma2006377 |*Macromolecules* 2011, 44, 5168–5177

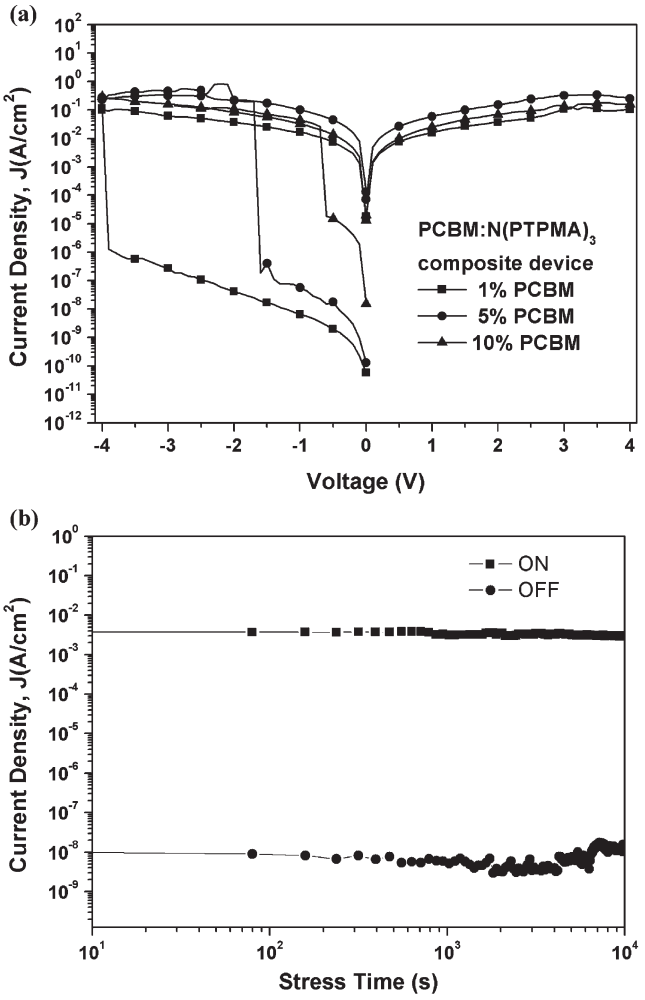

Figure 6. (a) Current density vs voltage plots for ITO/PCBM:N-(PTPMA)$_3$/Al composites devices. (b) Retention times of the ITO/1% PCBM:N(PTPMA)$_3$/Al. The read voltage of the memory devices was −1.0 V for the ON or OFF state.

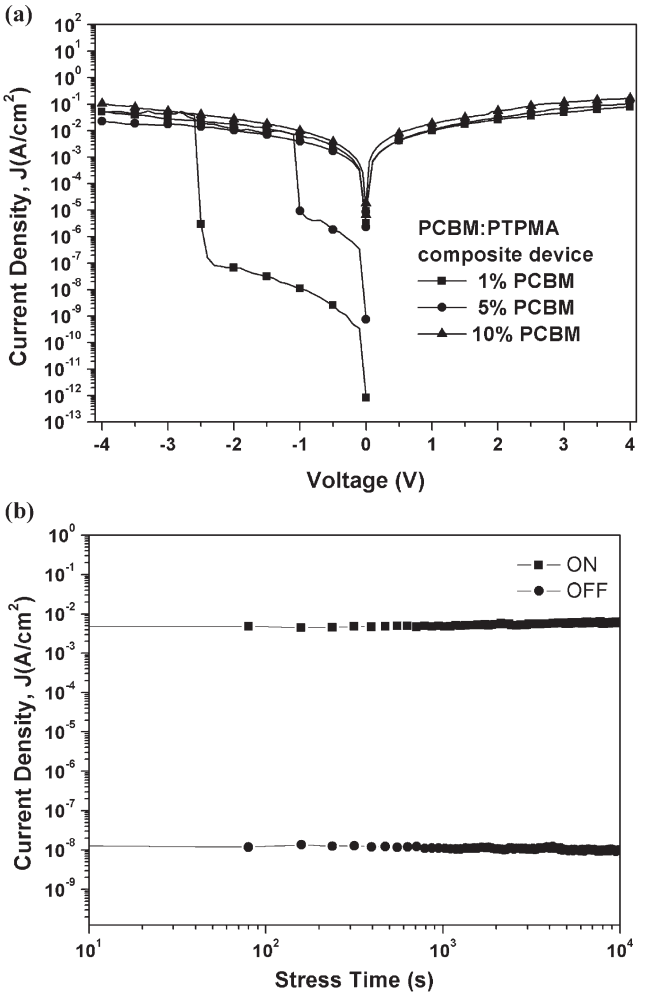

Figure 7. (a) Current density vs voltage plots for ITO/PCBM: PTPMA/Al composites devices. (b) Retention times of the ITO/1% PCBM:PTPMA/Al. The read voltage of the memory devices was −1.0 V for the ON or OFF state.

The pulse period and width are 3 and 2 μs, respectively. The N(PTPMA)$_3$ memory device is stable for at least 10^8 continuous read pulses of −1 V as shown in Figure 5c. Therefore, the switching and volatile behavior of pristine N(PTPMA)$_3$ memory device has a DRAM characteristic. The electrical memory device based on the linear PTPMA device also exhibits a DRAM characteristic similar to that of N(PTPMA)$_3$ based device, as shown in Figure S3 of the Supporting Information.

The current density−voltage ($J-V$) curves based on the PCBM: N(PTPMA)$_3$ composite devices are shown in Figure 6a. The film thickness of polymer composite layer, PCBM:N(PTPMA)$_3$, is similar to that of the pristine N(PTPMA)$_3$ device. The device based on 1%, 5%, or 10% PCBM:N(PTPMA)$_3$ composite thin film is first negative voltage swept scan from 0 to −4.0 V (sweep 1); the current density initially remains at a low conductance (OFF state). The current density increases abruptly and changes to a high conduction state at the threshold voltage (−3.9 V for 1% PCBM: N(PTPMA)$_3$; −1.5 V for 5% PCBM:N(PTPMA)$_3$; −0.8 V for 10% PCBM:N(PTPMA)$_3$), indicating the transition from the OFF state to the ON state as the "writing" process. The current density maintains at high conduction state (ON state) for the subsequent negative sweep from 0 to −4.0 V (sweep 2) and positive sweep from 0 to 4.0 V (sweep 3). The memory device could not return to the OFF state even after turning off the power or applying a reverse bias, suggesting the write-once-read-many-times (WORM) memory behavior. The ON/OFF current ratio was 10^6 (observed at −1 V for 1 or 5% PCBM:N(PTPMA)$_3$) and 10^3 (observed at −0.1 V for 10% PCBM:N(PTPMA)$_3$). The retention time tests on the above WORM memory devices for the OFF and ON states could remain over 10^4 s without obvious degradation, which suggests the excellent device stability as shown in Figure 6b and Figure S4 of the Supporting Information.

The $J-V$ curves of the corresponding device with the PTPMA and their PCBM composite films are exhibited in Figure 7a for comparison. The electrical characteristic of the 1% or 5% PCBM: PTPMA composite films exhibits the WORM memory behavior with different threshold voltage (−2.5 V for 1% PCBM:PTPMA, −1.0 V for 5% PCBM:PTPMA). The 1% and 5% PCBM:PTPMA memory devices exhibit excellent device stability for the ON or OFF state without obvious degradation over 10^4 s, as shown in Figure 7b and Figure S5 of the Supporting Information, respectively. However, the memory device of 10%PCBM:PTPMA composite film shows a conductor memory behavior. The current density is initially at a high conductance state and remains from the

dx.doi.org/10.1021/ma2006377 |*Macromolecules* 2011, 44, 5168–5177

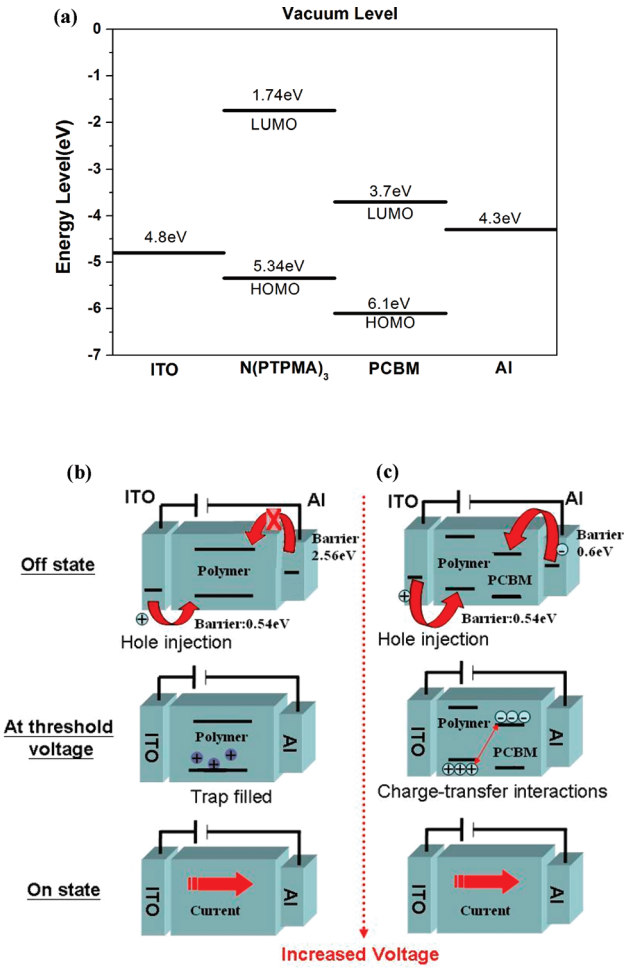

Figure 8. (a) Energy level diagram for the ITO/PCBM: $N(PTPMA)_3$/Al device. (b) Operating mechanism of the ITO/$N(PTPMA)_3$/Al device. (c) Operating mechanism of the ITO/PCBM:$N(PTPMA)_3$/Al device.

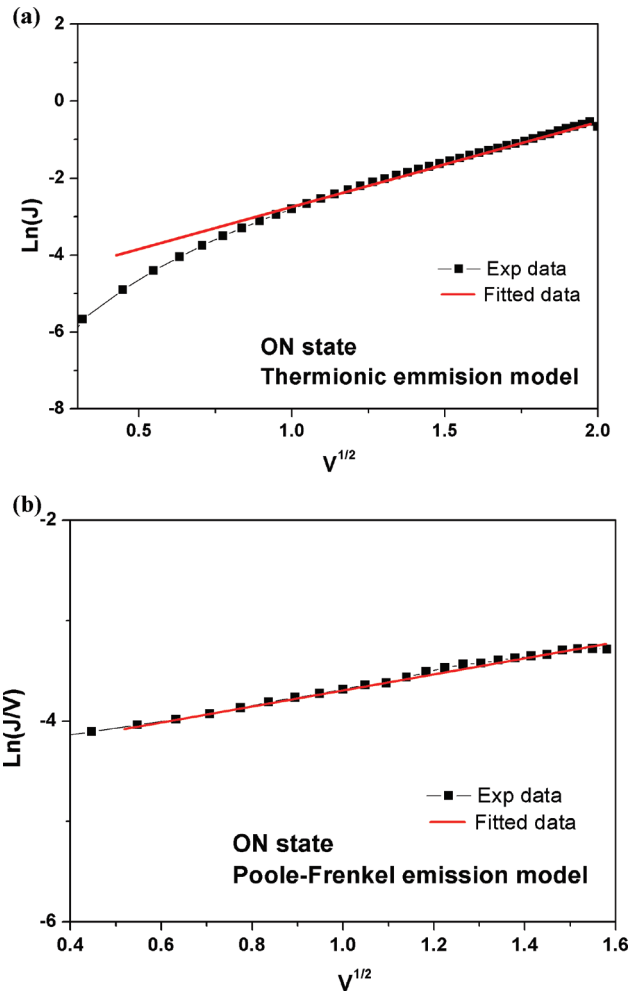

Figure 9. Analysis of fitted $J-V$ characteristics of the (a) ITO/$N(PTPMA)_3$/Al and (b) ITO/10%PCBM:$N(PTPMA)_3$/Al devices in the ON states.

negative sweep (0 to −4.0 V) and positive sweep (0 to 4.0 V). The different electrical characteristics of 10% PCBM composite films based on linear or star-shaped polymer indicate the significance of polymer architecture on the memory characteristics.

Memory Devices Mechanism of $N(PTPMA)_3$ and Its PCBM Composite. The memory behaviors of the $N(PTPMA)_3$ and PCBM:$N(PTPMA)_3$ composite films show DRAM and WORM characteristics, respectively. The energy level diagram of the studied materials is shown in Figure 8a. The work functions of two electrodes of the memory device are 4.3 and 4.8 eV for Al and ITO, respectively. On the other hand, the energy levels (HOMO, LUMO) of $N(PTPMA)_3$ and PCBM are (−5.34, −1.74) eV and (−6.1, −3.7) eV, respectively. The proposed operational mechanism of the ITO/$N(PTPMA)_3$/Al device is depicted in Figure 8b. In the ITO/$N(PTPMA)_3$/Al device, the pristine $N(PTPMA)_3$ is hole-transporting dominate due to the small energy barrier of ITO/HOMO (0.54 eV) compared to that of Al/LUMO (2.56 eV), which exhibits the p-type semiconductor characteristics. It is easier for the hole injected from ITO into HOMO of $N(PTPMA)_3$ and driven along the neighboring TPA moieties when applied negative voltage to the Al electrode. However, the excimer-forming sites of the $N(PTPMA)_3$ film observed from the PL spectra could be served as hole-trapping sites due to the new high-lying HOMO band or unexpected defects formation. The hole accumulation is suggested at near the electrode or trapped in the $N(PTPMA)_3$ layer with further increase in bias voltage.[46,47] Until the threshold voltage, the traps are filled and the current density abruptly increased. The trapped charges probably detrapped and redistributed without a continuous voltage bias, which leads the devices return to off state in the observed DRAM device. The plot of $\ln(J)$ vs $V^{1/2}$ for ITO/$N(PTPMA)_3$/Al device in the ON state can be fitted to a straight line. The charge transport-dominated ON state is confirmed by thermionic emission model as shown in Figure 9a, similar to those reported in the literature.[1]

The operational mechanism of the ITO/PCBM:$N(PTPMA)_3$/Al device is depicted in Figure 8c. The energy barriers between PCBM (LUMO) and Al is 0.6 eV, which is similar to that of $N(PTPMA)_3$ (HOMO) and ITO is 0.54 eV. Thus, the hole or electron injection barrier is similar under applied voltage. The current density remained at low conduction state under the initial voltage swept is probably due to the blocking of hole-transporting by the PCBM moiety. Above the threshold voltage, both of the hole and electron could overcome the energy barriers (~0.6 eV) and inject into the HOMO of the $N(PTPMA)_3$ and LUMO of PCBM, respectively. The charged HOMO of the $N(PTPMA)_3$ and the LUMO of PCBM form a conduction channel through

dx.doi.org/10.1021/ma2006377 |Macromolecules 2011, 44, 5168–5177

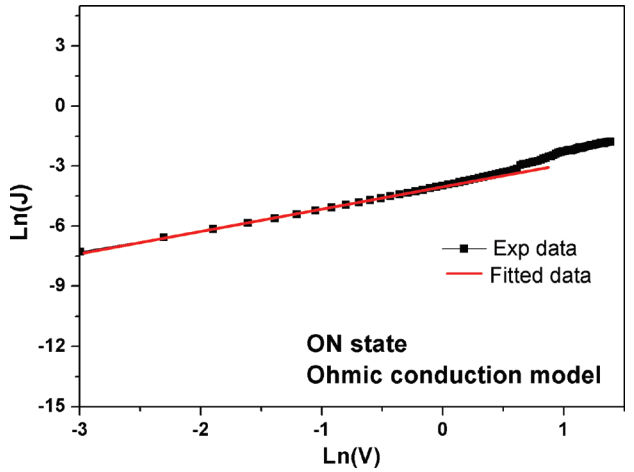

Figure 10. Analysis of fitted $J-V$ characteristics of the ITO/10% PCBM:PTPMA/Al device in the ON states.

charge-transfer interactions.[48] The charge stabilized in the PCBM:polymer composite films may not be easily removed even under the reverse field. The current density can be retained at a high conductance state for a long time in the observed WORM device. The threshold voltage decreases as the PCBM enhanced since it reduces the barrier for charge hopping.

The 10% PCBM composite films based on the linear or star-branched TPA polymers showed different type of on the memory characteristics. The plot of $\ln(J/V)$ vs $V^{1/2}$ for ITO/10% PCBM:N(PTPMA)$_3$/Al device in the ON state can be fitted to a straight line. The charge transport-dominated ON state is confirmed by Poole−Frenkel (PF) emission and could be fitted as shown in Figure 9b. However, the plot of $\ln(J)$ vs $\ln(V)$ for ITO/10% PCBM:PTPMA/Al device in the ON state can be fitted to a straight line with a slope 1.0 as shown in Figure 10, suggesting that the ohmic conduction is the charge transport-dominated mechanism. Larger aggregated size of PCBM cluster observed in the 10% PCBM:PTPMA composite film probably causes short circuits due to electrically connected channels formed between two electrodes. Besides, the higher turn-on voltage is observed in the PCBM:N(PTPMA)$_3$ device compared to PCBM:PTPMA device with the same PCBM content. The hole injection barrier from ITO to the linear or star-shaped polymer is similar. However, the steric hindrance of the star-shaped polymer architecture probably reduces the electron transport efficiency from Al to the LUMO of PCBM molecules. This study suggests the importance of polymer architecture or donor/acceptor composition for advanced memory device applications.

CONCLUSIONS

We have successfully synthesized well-defined linear and three-armed star-shaped polymers with pendent triphenylamine moieties by the GTP using the three-armed silyl ketene acetal initiator. The molecular weights and their distributions of the new TPA based polymer could be precisely controlled by the initiator/monomer ratio. The electrical memory characteristic of PCBM:N(PTPMA)$_3$ composite film based devices changed from DRAM to WORM, WORM, and WORM at the PCBM compositions of 0%, 1%, 5%, and 10%, respectively. The charge transport mechanism at ON state could be explained by thermionic emission model (DRAM device) and dominated Poole−Frenkel (PF) emission model (WORM device). The different polymer architecture of the PCBM composite thin film had the significant effect on charge transport properties such as turn-on voltage and conduction mechanism. The present study demonstrated the tunable electrical memory characteristics by polymer architecture or donor/acceptor composition for PCBM:polymer composites.

ASSOCIATED CONTENT

Supporting Information. ^{1}H NMR spectra of PTPMA (run 2) and N(PTPMA)$_3$ (run 6) in $CDCl_3$; AFM height images of 1% PCBM:N(PTPMA)$_3$, 5% PCBM:N(PTPMA)$_3$, 10% PCBM:N(PTPMA)$_3$, 1% PCBM:PTPMA, 5% PCBM:PTPMA, and 10% PCBM:PTPMA composite thin films; current density−voltage curves, retention times, and stimulus effect of read pulses on the ON and OFF states for ITO/PTPMA/Al devices; retention times of the ITO/5% PCBM:N(PTPMA)$_3$/Al and ITO/10% PCBM:N(PTPMA)$_3$/Al; retention times of the ITO/5% PCBM:PTPMA/Al. This material is available free of charge via the Internet at http://pubs.acs.org.

AUTHOR INFORMATION

Corresponding Author

*E-mail: chenwc@ntu.edu.tw (W.-C.C.); kakuchi@poly-bm.eng.hokudai.ac.jp (T.K.).

Author Contributions

‖J. C. Hsu and Y. Chen equally contributed to this work.

ACKNOWLEDGMENT

We especially thank for the financial support of this work from National Science Council (NSC), the Ministry of Economic Affairs, and the Excellence Research Program of National Taiwan University. Additionally, this study was partly supported by a Grant-in-Aid for the Japan Society for the Promotion of Science (JSPS) Fellows and by the Global COE Program (Catalysis as the Basis for Innovation in Materials Science) of the Ministry of Education, Culture, Sports, Science and Technology.

REFERENCES

(1) Pradhan, B.; Batabyal, S. K.; Pal, A. J. *J. Phys. Chem. B* **2006**, *110*, 8274.

(2) Liu, G.; Ling, Q.-D.; Teo, E. Y. H.; Zhu, C.-X.; Chan, D. S.-H.; Neoh, K.-G.; Kang, E.-T. *ACS Nano* **2009**, *3*, 1929.

(3) Chu, C. W.; Ouyang, J.; Tseng, J. H.; Yang, Y. *Adv. Mater.* **2005**, *17*, 1440.

(4) Laiho, A.; Majumdar, H. S.; Baral, J. K.; Jansson, F.; Osterbacka, R.; Ikkala, O. *Appl. Phys. Lett.* **2008**, *93*, 203309.

(5) Hsu, J.-C.; Liu, C.-L.; Chen, W.-C.; Sugiyama, K.; Hirao, A. *Macromol. Rapid Commun.* **2011**, *32*, 528.

(6) Liu, J.; Yin, Z.; Cao, X.; Zhao, F.; Lin, A.; Xie, L.; Fan, Q.; Boey, F.; Zhang, H.; Huang, W. *ACS Nano* **2010**, *4*, 3987.

(7) Tseng, R. J.; Huang, J.; Ouyang, J.; Kaner, R. B.; Yang *Nano Lett.* **2005**, *5*, 1077.

(8) Son, D. I.; Park, D. H.; Kim, J. B.; Choi, J.-W.; Kim, T. W.; Angadi, B.; Yi, Y.; Choi, W. K. *J. Phys. Chem. C* **2010**, *115*, 2341.

(9) Song, Y.; Ling, Q. D.; Lim, S. L.; Teo, E. Y. H.; Tan, Y. P.; Li, L.; Kang, E. T.; Chan, D. S. H.; Zhu, C. *IEEE Electron Device Lett.* **2007**, *28*, 107.

(10) Li, G. L.; Liu, G.; Li, M.; Wan, D.; Neoh, K. G.; Kang, E. T. *J. Phys. Chem. C* **2010**, *114*, 12742.

(11) Ling, Q.-D.; Liaw, D.-J.; Teo, E. Y.-H.; Zhu, C.; Chan, D. S.-H.; Kang, E.-T.; Neoh, K.-G. *Polymer* **2007**, *48*, 5182.
(12) Ling, Q.-D.; Liaw, D.-J.; Zhu, C.; Chan, D. S.-H.; Kang, E.-T.; Neoh, K.-G. *Prog. Polym. Sci.* **2008**, *33*, 917.
(13) Hoeben, F. J. M.; Jonkheijm, P.; Meijer, E. W.; Schenning, A. P. H. J. *Chem. Rev.* **2005**, *105*, 1491.
(14) Shirota, Y. *J. Mater. Chem.* **2000**, *10*, 1.
(15) Sivula, K.; Ball, Z. T.; Watanabe, N.; Fréchet, J. M. J. *Adv. Mater.* **2006**, *18*, 206.
(16) Melucci, M.; Barbarella, G.; Zambianchi, M.; Benzi, M.; Biscarini, F.; Cavallini, M.; Bongini, A.; Fabbroni, S.; Mazzeo, M.; Anni, M.; Gigli, G. *Macromolecules* **2004**, *37*, 5692.
(17) Economopoulos, S. P.; Andreopoulou, A. K.; Gregoriou, V. G.; Kallitsis, J. K. *Chem. Mater.* **2005**, *17*, 1063.
(18) Sugiyama, K.; Hirao, A.; Hsu, J.-C.; Tung, Y.-C.; Chen, W.-C. *Macromolecules* **2009**, *42*, 4053.
(19) Häussler, M.; Lok, Y. P.; Chen, M.; Jasieniak, J.; Adhikari, R.; King, S. P.; Haque, S. A.; Forsyth, C. M.; Winzenberg, K.; Watkins, S. E.; Rizzardo, E.; Wilson, G. J. *Macromolecules* **2010**, *43*, 7101.
(20) Stolka, M.; Pai, D. M.; Renfer, D. S.; Yanus, J. F. *J. Polym. Sci., Part A: Polym. Chem.* **1983**, *21*, 969.
(21) Snaith, H. J.; Whiting, G. L.; Sun, B.; Greenham, N. C.; Huck, W. T. S.; Friend, R. H. *Nano Lett.* **2005**, *5*, 1653.
(22) Deng, L.; Furuta, P. T.; Garon, S.; Li, J.; Kavulak, D.; Thompson, M. E.; Fréchet, J. M. J. *Chem. Mater.* **2005**, *18*, 386.
(23) Whiting, G. L.; Snaith, H. J.; Khodabakhsh, S.; Andreasen, J. W.; Breiby, D. W.; Nielsen, M. M.; Greenham, N. C.; Friend, R. H.; Huck, W. T. S. *Nano Lett.* **2006**, *6*, 573.
(24) Lee, C.-C.; Yeh, K.-M.; Chen, Y. *J. Polym. Sci., Part A: Polym. Chem.* **2008**, *46*, 7960.
(25) Ling, Q.-D.; Chang, F.-C.; Song, Y.; Zhu, C.-X.; Liaw, D.-J.; Chan, D. S.-H.; Kang, E.-T.; Neoh, K.-G. *J. Am. Chem. Soc.* **2006**, *128*, 8732.
(26) Liu, Y.-L.; Ling, Q.-D.; Kang, E.-T.; Neoh, K.-G.; Liaw, D.-J.; Wang, K.-L.; Liou, W.-T.; Zhu, C.-X.; Chan, D. S.-H. *J. Appl. Phys.* **2009**, *105*, 044501.
(27) Wang, K.-L.; Liu, Y.-L.; Lee, J.-W.; Neoh, K.-G.; Kang, E.-T. *Macromolecules* **2010**, *43*, 7159.
(28) Wang, K.-L.; Liu, Y.-L.; Shih, I. H.; Neoh, K.-G.; Kang, E.-T. *J. Polym. Sci., Part A: Polym. Chem.* **2010**, *48*, 5790.
(29) Kuorosawa, T.; Chueh, C.-C.; Liu, C.-L.; Higashihara, T.; Ueda, M.; Chen, W.-C. *Macromolecules* **2010**, *43*, 1236.
(30) Kang, B.-G.; Kang, N.-G.; Lee, J.-S. *Macromolecules* **2010**, *43*, 8400.
(31) Natori, I.; Natori, S.; Usui, H.; Sato, H. *Macromolecules* **2008**, *41*, 3852.
(32) Higashihara, T.; Ueda, M. *Macromolecules* **2009**, *42*, 8794.
(33) Bellmann, E.; Shaheen, S. E.; Grubbs, R. H.; Marder, S. R.; Kippelen, B.; Peyghambarian, N. *Chem. Mater.* **1999**, *11*, 399.
(34) Williams, P. E.; Moughton, A. O.; Patterson, J. P.; Khodabakhsh, S.; O'Reilly, R. K. *Polym. Chem.* **2011**, *2*, 720.
(35) Huttner, S.; Sommer, M.; Steiner, U.; Thelakkat, M. *Appl. Phys. Lett.* **2010**, *96*, 073503.
(36) Webster, O. W. In *New Synthetic Methods*; Springer: Berlin, 2004; Vol. 167, p 257.
(37) Georgiou, T. K.; Vamvakaki, M.; Patrickios, C. S.; Yamasaki, E. N.; Phylactou, L. A. *Biomacromolecules* **2004**, *5*, 2221.
(38) Themistou, E.; Patrickios, C. S. *Macromolecules* **2004**, *37*, 6734.
(39) Kakuchi, R.; Chiba, K.; Fuchise, K.; Sakai, R.; Satoh, T.; Kakuchi, T. *Macromolecules* **2009**, *42*, 8747.
(40) Fuchise, K.; Sakai, R.; Satoh, T.; Sato, S.-i.; Narumi, A.; Kawaguchi, S.; Kakuchi, T. *Macromolecules* **2010**, *43*, 5589.
(41) Natori, I.; Natori, S.; Sekikawa, H.; Ogino, K. *React. Funct. Polym.* **2009**, *69*, 613.
(42) Burkhart, R. D.; Jhon, N. I. *J. Phys. Chem.* **1991**, *95*, 7189.
(43) Burkhart, R. D.; Chakraborty, D. K.; Shirota, Y. *Macromolecules* **1991**, *24*, 1511.
(44) Park, M. H.; Huh, J. O.; Do, Y.; Lee, M. H. *J. Polym. Sci., Part A: Polym. Chem.* **2008**, *46*, 5816.
(45) Sary, N.; Richard, F.; Brochon, C.; Leclerc, N.; Lévêque, P.; Audinot, J.-N.; Berson, S.; Heiser, T.; Hadziioannou, G.; Mezzenga, R. *Adv. Mater.* **2010**, *22*, 763.
(46) Zhao, H.; Yuan, W. Z.; Tang, L.; Sun, J. Z.; Xu, H.; Qin, A.; Mao, Y.; Jin, J. K.; Tang, B. Z. *Macromolecules* **2008**, *41*, 8566.
(47) Kido, J.; Harada, G.; Komada, M.; Shionoya, H.; Nagai, K. In *Photonic and Optoelectronic Polymers*; American Chemical Society: Washington, DC, 1997; Vol. 672, p 381.
(48) Yokoyama, M.; Akiyama, K.; Yamamori, N.; Mikawa, H.; Kusabayashi, S. *Polym. J.* **1985**, *17*, 545.
(49) Ling, Q. D.; Lim, S. L.; Song, Y.; Zhu, C. X.; Chan, D. S. H.; Kang, E. T.; Neoh, K. G. *Langmuir* **2007**, *23*, 312.